Kalman filter-based tracking of moving objects using linear ultrasonic sensor array for road vehicles

CrossMark

Shengbo Eben Li [a,1], Guofa Li [b,*,1], Jiaying Yu [a], Chang Liu [c], Bo Cheng [a], Jianqiang Wang [a], Keqiang Li [a]

[a] State Key Lab of Automotive Safety and Energy, Department of Automotive Engineering, Tsinghua University, Beijing 100084, China
[b] Institute of Human Factors and Ergonomics, College of Mechatronics and Control Engineering, Shenzhen University, Shenzhen 518060, China
[c] Department of Mechanical Engineering, University of California, Berkeley, CA 94720, USA

A R T I C L E   I N F O

A B S T R A C T

Detection and tracking of objects in the side-near-field has attracted much attention for the development of advanced driver assistance systems. This paper presents a cost-effective approach to track moving objects around vehicles using linearly arrayed ultrasonic sensors. To understand the detection characteristics of a single sensor, an empirical detection model was developed considering the shapes and surface materials of various detected objects. Eight sensors were arrayed linearly to expand the detection range for further application in traffic environment recognition. Two types of tracking algorithms, including an Extended Kalman filter (EKF) and an Unscented Kalman filter (UKF), for the sensor array were designed for dynamic object tracking. The ultrasonic sensor array was designed to have two types of fire sequences: mutual firing or serial firing. The effectiveness of the designed algorithms were verified in two typical driving scenarios: passing intersections with traffic sign poles or street lights, and overtaking another vehicle. Experimental results showed that both EKF and UKF had more precise tracking position and smaller RMSE (root mean square error) than a traditional triangular positioning method. The effectiveness also encourages the application of cost-effective ultrasonic sensors in the near-field environment perception in autonomous driving systems.

© 2017 Elsevier Ltd. All rights reserved.

1. Introduction

With rapid development of advanced driver assistance systems (ADAS) and intelligent vehicles, various types of sensors (e.g., radars with79 GHz or 24 GHz, lidar, camera, ultrasonic sensor, etc.) have been utilized to percept the surrounding traffic environment of road vehicles [1,2]. Among these sensors, ultrasonic ones have the advantages of low cost, wide detection angle, small blind zone in the near-field and relatively good robustness to variant environmental conditions (e.g., lighting, fog, etc.) [3–6]. Additionally, the detection range of ultrasonic sensors can be significantly expanded from near-field (< 2 m) to middle-distance (5 m or even longer) by reducing signal attenuation and increasing the sensitivity of signal processing circuit [7] .

---

* Corresponding author.
 E-mail addresses: lisb04@gmail.com (S.E. Li), guofali@szu.edu.cn (G. Li), ljty10000n@sina.com (J. Yu), changliu@berkeley.edu (C. Liu), chengbo@tsinghua.edu.cn (B. Cheng), wjqlws@tsinghua.edu.cn (J. Wang), likq@tsinghua.edu.cn (K. Li).
 [1] The first two authors, Shengbo Eben Li and Guofa Li, have equally contributed to this research work.

Ultrasonic sensors apply the principle of 'time of flight' (TOF) to measure distance, which computes the travel time of ultrasonic echo reflected from the target [8]. Therefore, the performance of ultrasonic sensors highly depends on the reflective characteristics (e.g., shape, surface material) of the target surface. In urban traffic environments, traffic participants and road facilities are with various shapes and surface materials. For example, the shapes of vehicles and pedestrians are largely different from each other. The surface material of vehicles is metal, while that for pedestrians is usually cloth. Besides, variation of ultrasound speed due to fluctuations of temperature, humidity and wind may also have noticeable effects on the measurement accuracy [9], which complicates the analysis of ultrasonic signals.

Thus, an accurate and reliable model of ultrasonic sensors is of critical importance to the design of detection and tracking algorithms. In the literature, the models can be divided into two types based on their modeling principles: physical models and empirical models. The physical models are derived from the fundamentals of sensor working process, which simulate the errors based on the mechanisms of generation. For example, Kuc and Siegel designed a three-level model including geometric distance calculation, attenuation from reflection and transmission, and object recognition based on threshold methods [10]. A physical model has strong ability to predict sensing process; however, it is difficult to be adopted in traffic environment due to the hardness of ultrasound propagation simulation in unstable atmosphere and attenuation simulation from complex surfaces. The empirical model, by considering the ultrasonic sensor as a black box, interprets sensor measurements as outcomes of the underlying random process [11]. Building an empirical model usually requires various environments and large amounts of experiments, which discourages its applicability in the traffic environments [12]. Some empirical models only focus on the observable performance metrics, for example, detection range and measurement error, which are more environmentally flexible and can be generated through a few experiments. For example, Ishihara et al. built a deterministic sensor model with ranging accuracy influenced by object orientations, and discovered that object orientation could affect the ranging accuracy up to 3% [13]. Majchrzak et al. developed a deterministic sensor model based on experimental results with measurement error related to target distance [14]. These models consider a few factors like target distance and orientation. In this study, we build a new deterministic model that incorporates additional factors such as target shape and target surface material to extend its suitability in traffic environment.

Using ultrasonic sensor models with good accuracy and reliability, arrayed sensors could be employed to localize and track objects. Existing methods on object localization and tracking can be classified into two categories: deterministic methods and probabilistic methods. Deterministic methods usually utilize the spherical positioning technique for object localization, which computes the intersection area of circles centered at each sensor with radius equal to the measured distance [15]. The triangle method is a representative using the framework of deterministic methods, cooperating measures from two sensors for two dimensional positioning. These methods are relatively simple to implement but do not take the uncertainty of sensor into consideration. Probabilistic methods, on the other hand, represent information in a probabilistic way [16]. Common approaches include nonparametric filters and parametric filters. Nonparametric filters such as histogram filter and particle filter decompose the state space probability distribution into a histogram and a series of particles respectively. Köhler et al. set up a linear sensor array with three sensors mounted on both sides of a vehicle and utilized the particle filter to track objects [17]. Joint particle weighting was decided by an inverse sensor model and a reliability model. Yang developed an improved partible filter using a four fixed features based system model to limit the density of the landmarks and as well as the computing complexity [18]. Above that, a map adjustment technique was used to increase the accuracy and efficiency of the tracking algorithm. Other examples can be found in Adiprawita et al. [19], Zhang and Zapata [20] and Muller [21]. Such nonparametric filters as particle filters have good tracking performance on nonlinear sensing dynamics, yet it incurs high computation burden when large number of particles are needed to ensure tracking precision. The case is even severe in arrayed sensors when multiple sensor measurements are utilized at each step. In contrast, the parametric filter based tracking approaches, including Kalman filter, Extended Kalman filter and Unscented Kalman filter, use time-varying parameters to represent probability distribution and are well suited for continuous tracking with low computational complexity in dynamic environment. D'Alfonso et al. set up a sectorial sensor array with five ultrasonic sensors and utilized EKF and UKF which contains a switching sensor activation policy for indoor position and orientation estimating [22]. A substantial equivalence of the two filters was showed by real data based tracking results. Ko and Choi developed an UKF for indoor object localization, which used a pre-filtering method to overcome the bad effect from unexpected external noise [23]. Kim SJ and Kim BK used isotropic ultrasonic Tx and Rx array for the tracked object and the tracking platform separately [24]. An EKF is developed to compensate the ultrasonic distances from the odometric information traveled by the platform. Beyond that, Extended Kalman filter and Unscented Kalman filter are also capable in sensing systems with nonlinear dynamics and are therefore be adopted in this work for object tracking in traffic environment.

This paper aims to: 1) develop an accurate and reliable ultrasonic sensor model for traffic environment recognition considering the shapes and surface materials of traffic participants and road facilities; and 2) design object tracking algorithms using linearly arrayed ultrasonic sensors and compare their tracking performances to the triangle positioning method. The main contribution of this paper lies in the successful attempts to track surrounding objects dynamically in traffic environments using improved Kalman filtering algorithms based on cost-effective ultrasonic sensor array. This work also encourages the application of cost-effective ultrasonic sensors in the near-field environment perception in fuel consumption strategies [25] and autonomous driving systems.

2. Modeling of single ultrasonic sensor

2.1. Experiment design

An experiment platform was constructed to analyze the characteristics of single ultrasonic sensor. As shown in Fig. 1, the platform consisted of three main components: an ultrasonic sensor, the control circuit and a personal computer (PC). The control circuit was based on the Arduino board and could actuate the sensor module by sending out a series of pulses and then captured the echoes to calculate the distance. The temperature module in the control circuit was based on the non-contact infrared sensor module MLX90614, which was used to compensate for the effect of temperature fluctuation. The communication between the platform and the PC was realized using serial connection.

This experiment aims to understand the measurement accuracy for different objects that may appear in a vehicle's side zone using ultrasonic sensors. Four characteristics of the objects were considered, including object shape, surface material, relative distance to the sensor and relative orientation to the center line of the sensor. The relative distance between the object and the sensor center ranged from 0.5 m to 5 m with an interval of 0.5 m. The orientation to the center line of the sensor ranged from −60° to 60° with an interval of 10°. See Fig. 2 for the layout of the experiment.

Traffic participants and road facilities were categorized into groups according to their shape and surface material attributes. For example, according to their shape, poles or boles by the side of roads were recognized as thin rods, humans and big tree boles as thick rods, and vehicles as flat surfaces. Similarly, they were categorized into metal, polyvinyl chloride (PVC) plastic and cloth groups according to the surface material. See Fig. 3. Thus, 9 kinds of objects (3 shapes × 3 surface materials) were tested using the same ultrasonic sensor on the detection performance at different positions as illustrated in Fig. 2. This categorization method covered most of the traffic participants and road facilities in the real city-traffic environment.

2.2. Experiment data analysis

The probability for an object to be detected by ultrasonic sensors (namely chance of detection) at different positions is illustrated in Fig. 4. The results for PVC thin rod objects are shown in Fig. 4(b). When the rods moved further from the ultrasonic sensor, the chance of detection decreased sharply when the distance to the sensor exceeded 2.0 m at 0° to the center line of the sensor. Similar trends were found when the angle to the center line of the sensor was 10 or 20°. Interestingly, wherever the PVC thin rod was placed at any distance with an angle larger than 30°, the chance of detection lost, keeping at 0. Almost the same thing happened for the detection of other types of objects. See Fig. 4 for details.

2.2.1. Detection scope model by single sensor

The detection scopes for each kind of objects are illustrated in Fig. 5. The warmer the color is, the higher probability a specific object would be detected. Objects within the innermost red line can be detected with a 100% probability, while objects outside the outermost blue line will never be detected. The probability to be detected decreases within the colored region, from the innermost to the outermost. Results showed that the detection performance for metal objects ranked the highest with PVC ranking the second and cloth ranking the third. For the detection performance of objects with different shapes, flat surface ranked the highest, following by thick rod and thin rod. In this paper, we define the effective detection
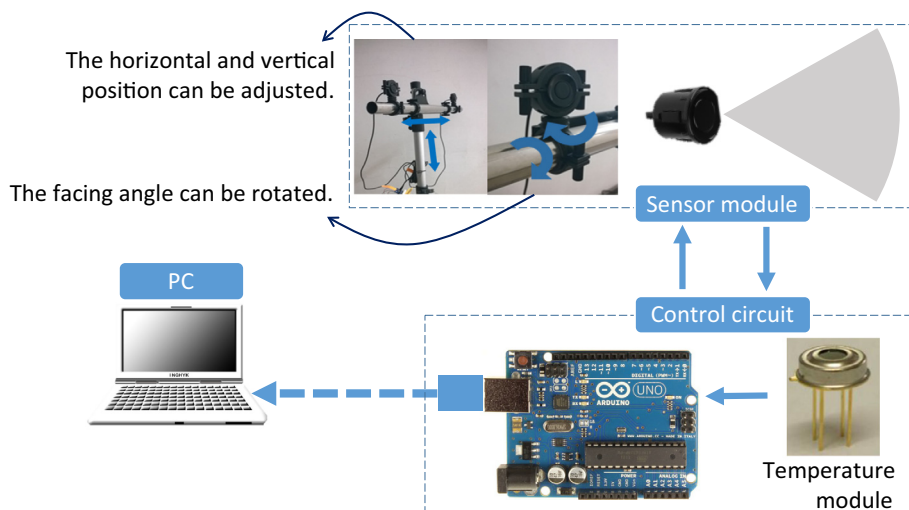

The horizontal and vertical position can be adjusted.

The facing angle can be rotated.

Sensor module

PC

Control circuit

Temperature module

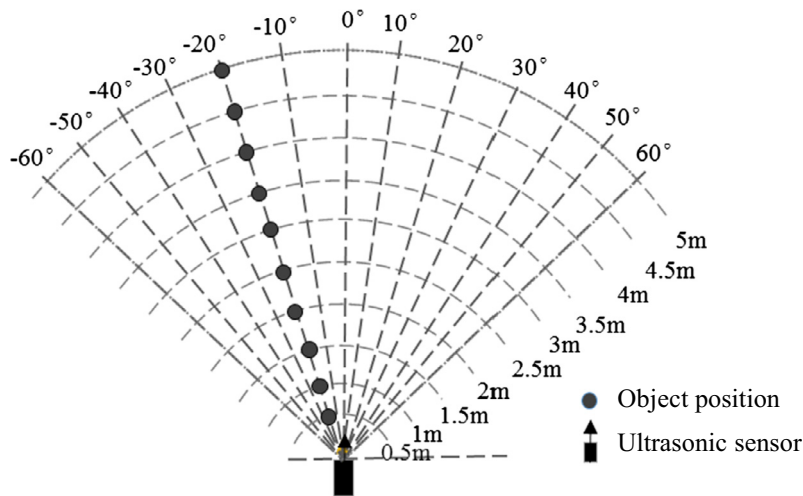**Fig. 1.** Configuration of the experiment platform.

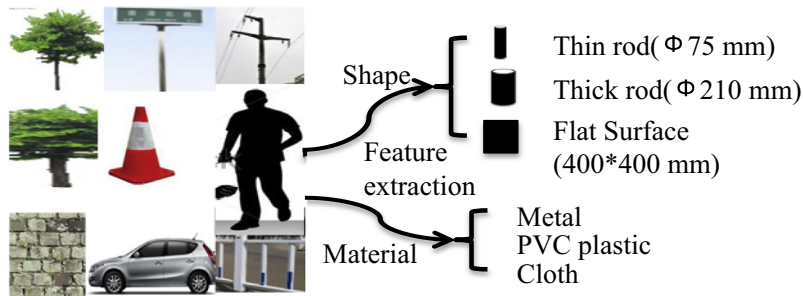**Fig. 2.** Experiment design.

Fig. 3. Classification of tested objects.

scope as the region in which the detection probability is 100% and the maximum detection scope as the region with a detection probability of 0.

To fit the detection scopes illustrated in Fig. 5, three planar geometry models were employed. They were an ellipse, a half ellipse + a triangle, and two quadratic curves. The illustrated models, mathematical equations and parameter values for each model can be found in Table 1.

Root Mean Square Error (RMSE) was adopted as the criteria to compare the performance of the three employed models. The smaller, the better. The performance results of the three models are shown in Fig. 6.

As presented, the two quadratic curves model was found to perform the smallest RMSE. The ellipse model ranked the second, and the half ellipse + a triangle model ranked the third. The fitting parameters of the two quadratic curves model for the detection of different object types are shown in Table 2, for both the effective detection scope and maximum detection scope. This model was used in the development of a detection probability model and further object tracking algorithms.

2.2.2. Measurement error model by single sensor

The fitting result between the measured and real distances of a thick rod is illustrated in Fig. 7(a). The measurement error is quite small and is subject to a normal distribution. See Fig. 7(b). Measurement error of ultrasonic sensors mainly comes from temperature fluctuation, wind speed disturbance and random noises. See Eq. (1) for the measurement error model. The sensors used in this study are with temperature compensation, and the tests were conducted in a sunny day with slight wind speed. Thus, the influence from temperature and wind could be neglected ($d_u \approx 0$), and the random error ε come out as the leading contributor to the measurement error.

$$d_t = d_0 + d_u + \varepsilon \tag{1}$$

It is assumed that the random error ε is a zero-mean Gaussian random variable. The random error is mainly influenced by the object shape, material, distance and orientation to the ultrasonic sensor. The errors with respect to the mentioned influencing factors are shown in Fig. 8. Linear regression was conducted to reveal the effects of these factors. As the object shapes and surface materials are discrete variables, regression needs to be conducted for objects with different shapes and materials. It
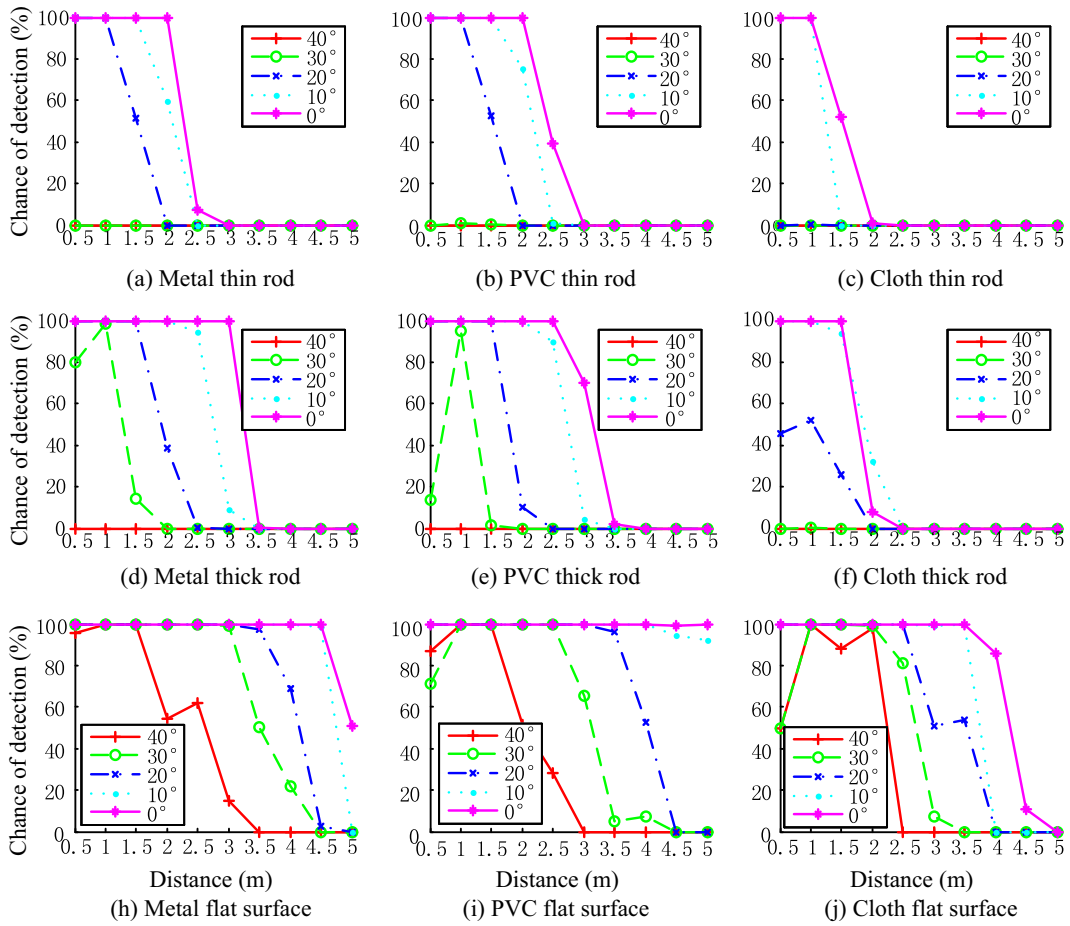
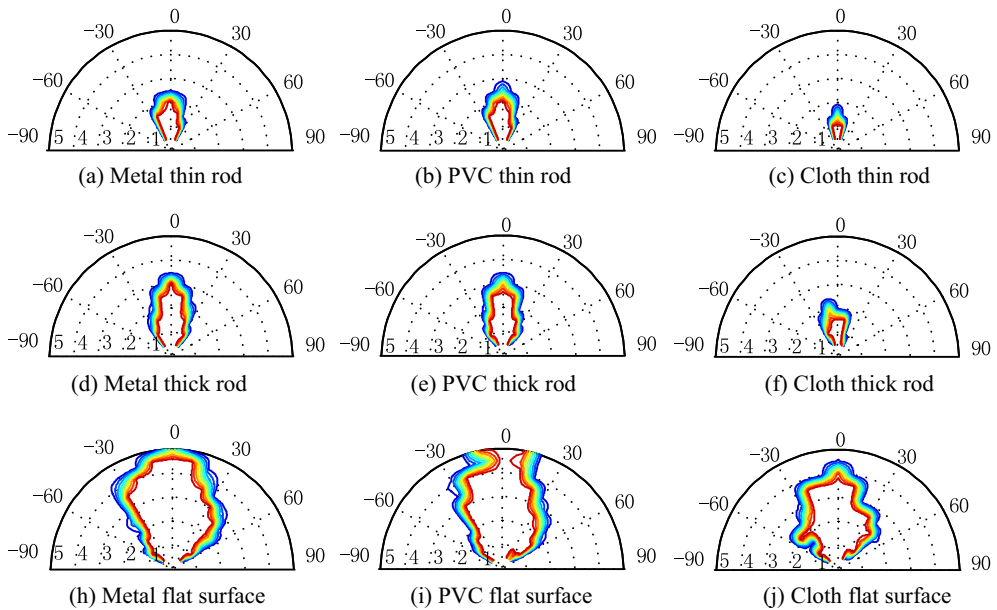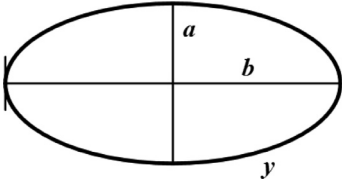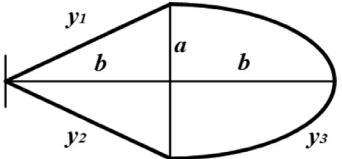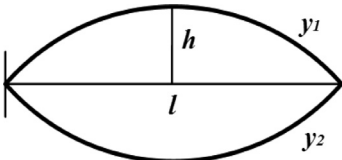Fig. 4. Chance of detection for PVC thin rod and metal thin rod.

Fig. 5. Detection scope of the ultrasonic sensor.

Table 1
Employed fitting models.

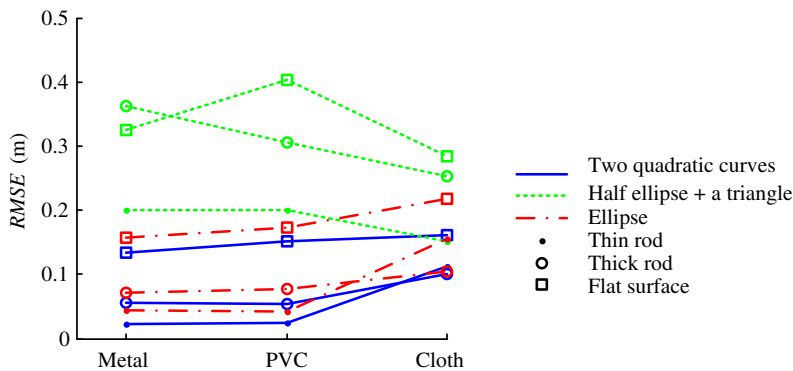| Fitting models		Equation	Parameter value
Ellipse		$x^2 + By^2 + Cy^2 = 0$	$B = \frac{a^2}{b^2}, \ C = -\frac{2a^2}{b}$
Half ellipse + a triangle		$y_1 = k_1 x y_2 = k_2 x$ $x^2 + By_3^2 + Cy_3 = 0$	$k_1 = -\frac{a}{b}, \ k_2 = \frac{a}{b}$ $B = \frac{a^2}{b^2}, \ C = -\frac{2a^2}{b}$
Two quadratic curves		$y_1^2 + By_1 + Cx = 0$ $y_2^2 + By_2 - Cx = 0$	$B = -l, \ C = -\frac{l^2}{4h}$

Fig. 6. Performance of the employed fitting models.

Table 2
Parameters of the two quadratic curves model for the detection of different objects.

Effective/Maximum		Metal	PVC	Cloth
Thin rod	l	2.05/2.71	2.09/2.97	1.09/1.98
	h	0.37/0.72	0.35/0.69	0.37/0.31
Thick rod	l	3.04/3.61	2.683.54	1.62/2.24
	h	0.56/0.98	0.54/0.86	0.35/0.79
Flat surface	l	4.89/5.42	4.98/5.70	3.80/4.63
	h	1.45/2.37	1.32/2.21	1.15/1.84

can be inferred from the previously obtained knowledge that the measurement errors change with a similar trend between objects with different shapes and materials. Thus, the proposed linear regression model is shown as:

$$SV = \beta_0 + \beta_1 d + \beta_2 \theta \tag{2}$$

where SV is the sample variance of measurement error ε, d is the distance (m), θ is the orientation to sensor central line (°, $\theta > 0$). The regression results show that $\beta_1 = 0.0795$, $\beta_2 = 0.0047$. β_0 varies with respect to different object shapes and surface materials. See Table 3 for the values of β_0.
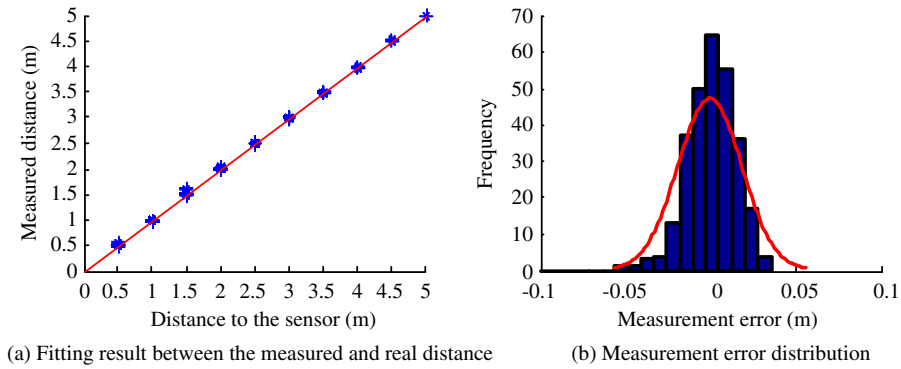
(a) Fitting result between the measured and real distance

(b) Measurement error distribution

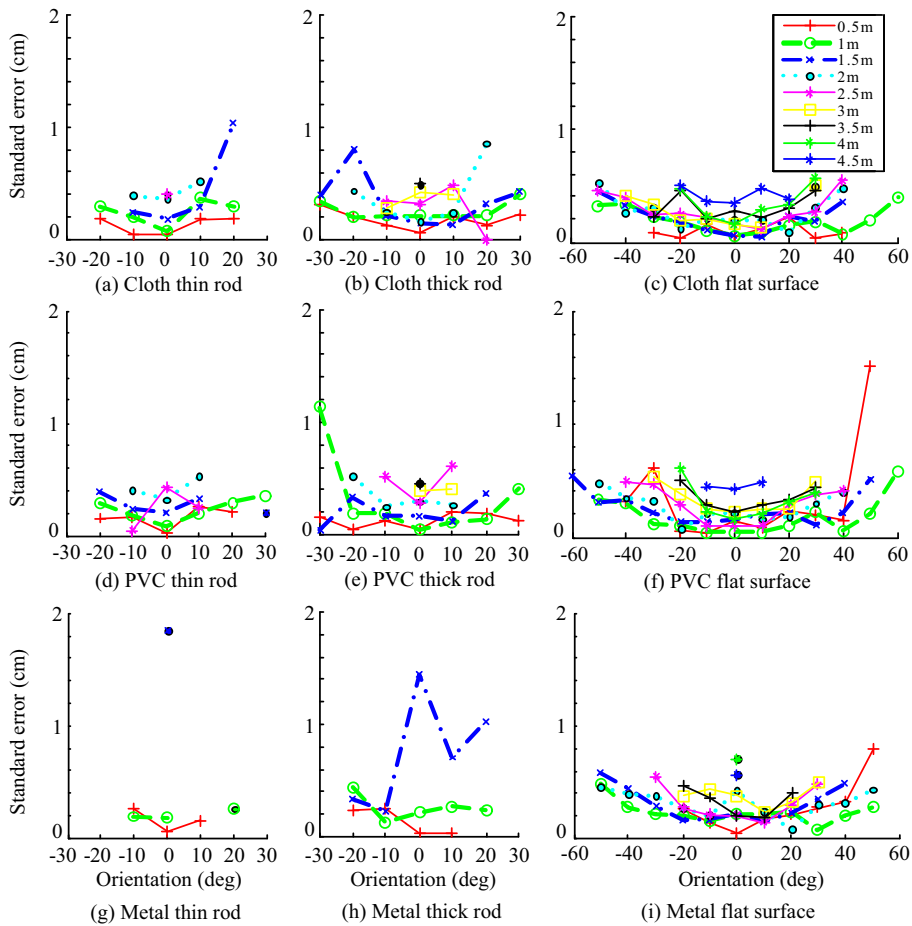**Fig. 7.** Measurement error analysis – case of a thick rod.

Fig. 8. Standard error of the measurements.

Table 3
Values of for different object shapes and surface materials.

	Metal	PVC	Cloth
Thick rod	0.0836	0.0863	0.0796
Thin rod	0.0670	0.0434	0.0691
Flat surface	−0.0474	−0.0352	0.0213

3. Design of two tracking algorithms using sensor array

To get a clear overview of the work presented this paper, the summarized structure is shown in Fig. 9. Single sensor modeling considering shapes and surface materials is marked as black lines. Measurement error model, detection scope model and detection probability model were built based on the work presented in Section 2. The proposed EKF and UKF tracking algorithms were presented in detail in Section 3. Verification of the proposed tracking algorithms were marked as green lines for the simulation, and red lines for the field tests. In the simulation, sensor measurement was simulated by employing the detection scope model and detection probability model. Simulated sensor measurement and measurement error model were used to verify the effectiveness of the proposed tracking algorithms. The results were shown in Section 4. In the field tests, measurement from the mounted sensors on the instrumented vehicle and the measurement error model served as inputs to verify the effectiveness of the proposed tracking algorithms. The results were shown in Section 5. Marked as dash lines in Fig. 9, object classification algorithm and application in advanced driver assistance systems (ADAS) or autonomous vehicles were not described in detail in this paper. The work on object classification algorithm design will be published in a further journal paper. Here in this paper, the object type was considered to be known, focusing on the tracking algorithms design and verification.

3.1. Configuration of arrayed ultrasonic sensors

Because of the detection scope limitation of a single ultrasonic sensor, multiple ones are needed for applications in vehicles to detect and track surrounding object. The arrayed ultrasonic system used in this study is presented in Fig. 10. On each side of the vehicle, 8 sensors with an interval of 50 cm between each were arrayed linearly to localize and track objects in the specific side zone. Two typical firing sequences were applied: serial sensor firing and mutual sensor firing. Serial sensor firing activates the sensor one by one, which requires only simple circuits but can result in less frequent measurements. Mutual sensor firing has the distinctive advantage of larger information content, while at the cost of more complex circuits and higher computation workload. See Fig. 11 for the illustration of firing sequences. In the serial firing sequence method, pair
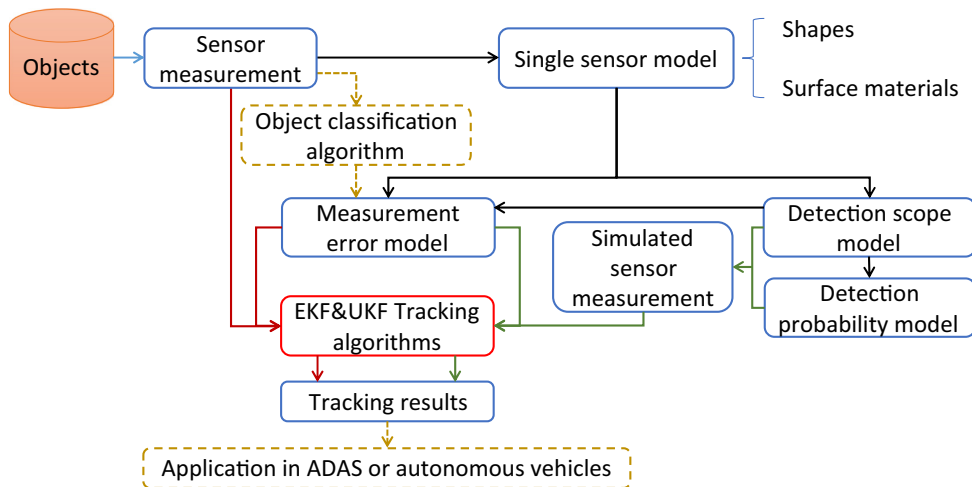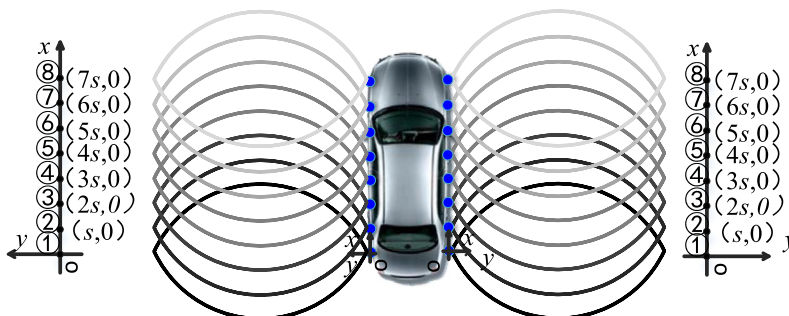

Fig. 9. The summarized structure of this paper.

Fig. 10. Sensor array system layout (s: distance between each two adjacent sensors).
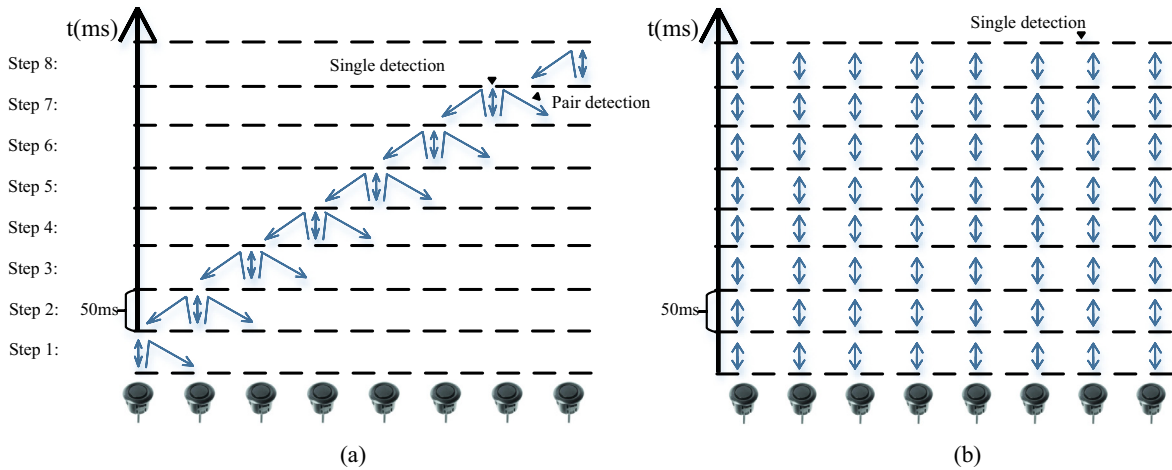
Fig. 11. (a) Serial sensor firing sequence; (b) Mutual sensor firing sequence.

detection were used. Pair detection means that when a sensor is fired, the firing sensor itself and the two adjacent sensors (one for the first and eighth sensor) are activated to receive the echo. See Fig. 11(a). The firing period *T* was set to 50 ms to ensure that no echo from the last pulse would be received. In the mutual firing sequence method, cross talking between different sensors may cause measurement errors. To solve this problem, many solutions have been proposed and validated [3,26] . The ultrasonic sensors used in this study have embedded the cross talking solution proposed by Agarwal et al. in the design of the sensory system [3].

3.2. Selection of typical tracking scenarios

Two typical tracking scenarios were examined. See Fig. 12. In scenario 1, a metal pole with a diameter of 20 cm was used to simulate the traffic sign or street light rods. The lateral distance between the pole and the host vehicle was 2 m. The host vehicle travelled at 5 km/h to detect and track the target pole. In scenario 2, another car with a lateral distance of 2 m to the host vehicle was travelling at 10 km/h to simulate an overtaking situation. The host vehicle still moved at 5 km/h. The vehicles were simulated as 4 × 1.8 m rectangles. As shown in Fig. 12, the sensor nearest to the end of the host vehicle was taken as the coordinate origin.

3.3. Tracking algorithm based on Kalman filter

The system model and observation model were established according to the kinematic movement characteristics in the typical scenarios. An Extended Kalman Filtering (EKF) and a Unscented Kalman Filter (UKF) tracking algorithms were designed based on the established observation model. The main challenges of the tracking algorithm design lie in the low firing frequency of the used sensors and the partially resulting limited effective signals in dynamically changing environments. Conventional methods cannot deal with this problem effectively, while tracking filters design has shown good capabilities in deal with it in dynamically changing environments. However, current attempts mainly focuses on the applications in robots. Solutions to the problems in automotive engineering need to be further developed.
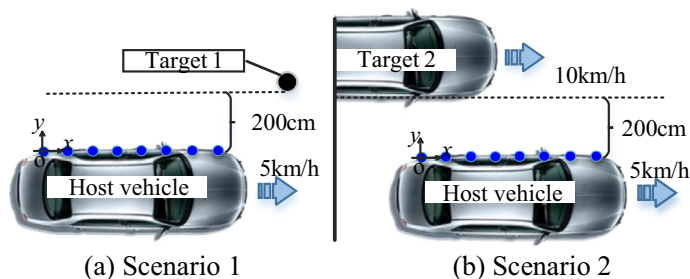

Fig. 12. Illustration of the two typical tracking scenarios.

3.3.1. System model and observation model

In this study, the sensors would be fired every 50 ms. Therefore, the arrayed sensor system could be regarded as a discrete system. The linearly moving trajectory shown in Fig. 12 indicates that the state transition matrix is a linear matrix. Although the observation matrix is linear in polar coordinate system, it would be nonlinear when converted to Cartesian coordinate system. Thus, the system model and observation model can be described as:

$$\begin{aligned} X_k &= AX_{k-1} + W_{k-1}, \\ Z_k &= h(X_k) + V_k, \end{aligned} \tag{3}$$

where X_k is the system state at time step k, Z_k is the observation vector at time step k, A is the status transition matrix, $h(\cdot)$ is the observation model, W_k, V_k are the independent zero-mean Gaussian process noise and observation noise, respectively. The system state is described as:

$$X_k = (x, y, v_x, v_y, a_x, a_y, \dot{a}_x, \dot{a}_y), \tag{4}$$

where x, y are the longitudinal and lateral position of the target objects, v_x, v_y are the traveling velocities, a_x, a_y are the accelerations, and $\dot{a}_x, \dot{a}_y$ are the derivative of accelerations. For the target tracking pole, it is regarded as a point. While for the target tracking vehicle, state variables of the front right point are used to describe the state information of the vehicle. The state transition matrix is:

$$A = \begin{bmatrix} 1 & 0 & T & 0 & T^2/2 & 0 & T^3/6 & 0 \\ 0 & 1 & 0 & T & 0 & T^2/2 & 0 & T^3/6 \\ 0 & 0 & 1 & 0 & T & 0 & T^2/2 & 0 \\ 0 & 0 & 0 & 1 & 0 & T & 0 & T^2/2 \\ 0 & 0 & 0 & 0 & 1 & 0 & T & 0 \\ 0 & 0 & 0 & 0 & 0 & 1 & 0 & T \\ 0 & 0 & 0 & 0 & 0 & 0 & 1 & 0 \\ 0 & 0 & 0 & 0 & 0 & 0 & 0 & 1 \end{bmatrix} \tag{5}$$

where T is the firing period of the sensors. The observation model for mutual firing sequence method is defined as:

$$h_i(X_k) = \sqrt{(x_i - x)^2 + (y_i - y)^2} \tag{6}$$

where (x_i, y_i) is the location of sensor i, (x, y) is the location of the tracking point. While the observation model for serial firing sequence method is defined as:

$$h_i(X_k) = \left(\sqrt{(x_i - x)^2 + (y_i - y)^2} + \sqrt{(x_j - x)^2 + (y_j - y)^2} \right)/2, \tag{7}$$

where (x_i, y_i) is the location of the receiving sensor i, (x_j, y_j) is the location of the firing sensor j, (x, y) is the location of the tracking point.

3.3.2. EKF (Extended Kalman Filtering) algorithm

The EKF utilizes Taylor Truncation to linearize the observation model with nonlinear observation. The linearized observation equation can therefore be described as:

$$H_{k,i} = \frac{\partial h_{k,i}(x)}{\partial x}\Big|_{x=\hat{X}_{k,i}^-}. \tag{8}$$

Due to the detection range limitation of the ultrasonic sensors, there will usually be some missing measurements among the 8 sensors. The detection probability model mentioned above in Section 2 was used to deal with this situation in the simulation work in Section 4. To track the target object effectively based on the available measurements, a centralized EKF method that selectively fuses valid measurements is developed. See Fig. 13. Suppose there are $m(1 \leqslant m < 8)$ sensors with valid measurements. The new observation vector and observation matrix are:

$$\begin{aligned} Z_{k,s} &= \left[Z_{k,s_1}, \ldots, Z_{k,s_m} \right]^T, \\ H_{k,s} &= \left[H_{k,s_1}, \ldots, H_{k,s_m} \right]^T. \end{aligned} \tag{9}$$

For sensors with valid measurements, target object position can be iteratively estimated as follows:
State prediction:

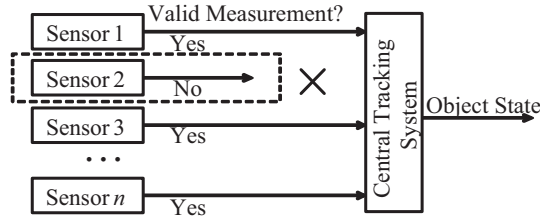$$\begin{aligned} \hat{X}_k^- &= A\hat{X}_{k-1}, \\ P_k^- &= AP_{k-1}A^T + Q. \end{aligned} \tag{10}$$

Fig. 13. Centralized Extended Kalman Filter (EKF) framework.

State update:

$$K_k = P_k^- H_{k,s}^T (H_{k,s} P_k^- H_{k,s}^T + R)^{-1},$$
$$\hat{X}_k = \hat{X}_k^- + K_k \left(Z_{k,s} - H_{k,s} \hat{X}_k^- \right),$$
$$P_k = \left(I - K_k H_{k,s}^T \right) P_k^-,$$

(11)

where $\hat{X}_k^-$ is the prior state estimate; $\hat{X}_k$ is the posterior state estimate.

The EKF uses Taylor's quadratic truncation to linearize the nonlinear systems [27]. As Taylor's quadratic truncation would bring large errors and weaken the EFK performance in the strong nonlinear systems, this method is limited to the applications in weak nonlinear situations with Gaussian characteristics. For systems with strong nonlinear characteristics, improved methods need to be developed.

3.3.3. UKF (Unscented Kalman Filter) tracking algorithm design

Although EKF is a standard technique adopted in a number of nonlinear estimation and machine learning applications, Wan and Van Der Merwe pointed out the flaws in using EKF and proposed an improved method using UKF [27]. In the EKF, the state distribution is approximated by a Gaussian random variable. It is then propagated analytically through the first-order linearization of the nonlinear system. This would introduce large errors which may lead to sub-optimal performance and divergence of the filter. The UKF addresses this problem by utilizing a polynomial approximation approach [28]. It is based on deterministic sampling methods (Unscented Transformation), which generates sampled sigma points to meet the mean and covariance of estimates from the last step. A normal method of symmetric sampling is utilized in this paper. The sampling process is shown as:

$$\begin{cases} \sum_{i=0}^{2r} w_i = 1 \\ \sum_{i=0}^{2r} w_i \chi_i - \bar{x} = 1 \\ \sum_{i=0}^{2r} w_i (\chi_i - \bar{x})(\chi_i - \bar{x})^T = P_{xx} \end{cases}$$

(12)

where r is the dimension of the sampling subject x (in this paper $r = 8$), $\bar{x}$ and P_{xx} represent the mean and covariance of x respectively, χ_i is the sampled point i, w_i is the weighting factor of sample i. The sampled points are:

$$\{\chi_i\} = \left[\bar{x} \bar{x} + \gamma \sqrt{P_{xx}} \bar{x} - \gamma \sqrt{P_{xx}} \right]$$

(13)

where $\gamma = \sqrt{r + \kappa}$, κ is the ratio parameter which adjusts the distance of the sigma points to $\bar{x}$. The weighting factors are:

$$w_i = \begin{cases} \kappa/(r + \kappa), i = 0 \\ 1/2(r + \kappa), i \neq 0 \end{cases}$$

(14)

For sensors with valid measurements, object position can be iteratively estimated as follows:

(1) State prediction:

$$\hat{\chi}^i(k+1|k) = A\chi^i(k|k),$$
$$\hat{X}(k+1|k) = \sum_{i=0}^{L-1} w_i^m \hat{\chi}^i(k+1|k),$$
$$P(k+1|k) = \sum_{i=0}^{L-1} w_i^c \left(\hat{\chi}^i(k+1|k) - \hat{X}(k+1|k) \right) \left(\hat{\chi}^i(k+1|k) - \hat{X}(k+1|k) \right)^T.$$

(15)

where is the sample number and $L = 2r + 1$. During state updating process, the observation vector and the observation matrix of the sensors with valid measurements are:

$$Z_{k,s} = \left[Z_{k,s_1}, \ldots, Z_{k,s_m}\right]^T,$$
$$h_{k,s} = \left[h_{k,s_1}, \ldots, h_{k,s_m}\right]^T. \tag{16}$$
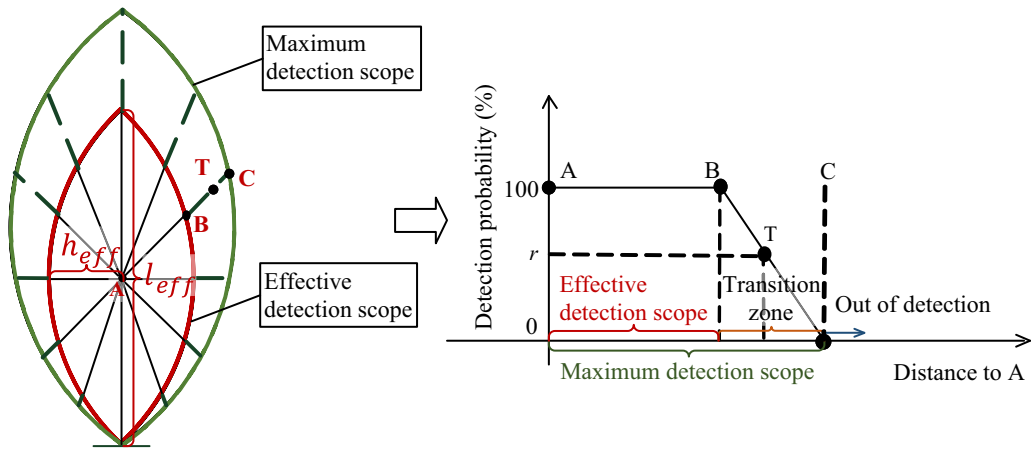
Fig. 14. Detection probability model of a single ultrasonic sensor.

(a) Lateral position

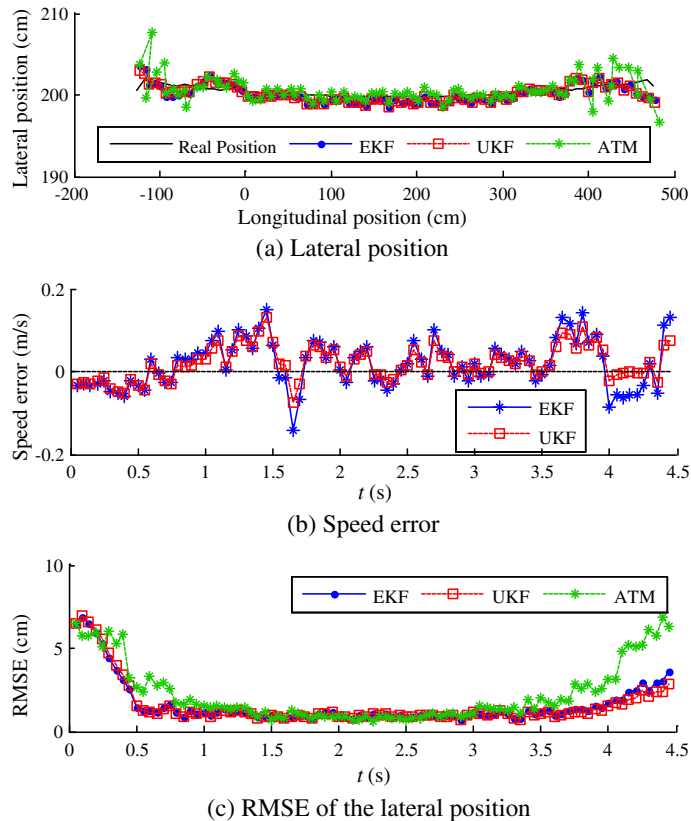(b) Speed error

(c) RMSE of the lateral position

Fig. 15. Tracking performance of mutual firing sequence in scenario 1.

(2) State update:

$$
\begin{aligned}
&\hat{Z}^i(k+1|k) = h_s(\hat{\chi}^i(k+1|k)), \\
&\hat{Z}(k+1|k) = \sum_{i=0}^{L-1} w_i^m \hat{Z}^i(k+1|k), \\
&P_{zz}(k+1|k) = \sum_{i=0}^{L-1} w_i^c (\hat{Z}^i(k+1|k) - \hat{Z}(k+1|k))(\hat{Z}^i(k+1|k) - \hat{Z}(k+1|k))^T, \\
&P_{xz}(k+1|k) = \sum_{i=0}^{L-1} w_i^c (\hat{Z}^i(k+1|k) - \hat{Z}(k+1|k))(\hat{Z}^i(k+1|k) - \hat{X}(k+1|k))^T, \\
&K(k+1) = P_{xz}(k+1|k)P_{zz}^{-1}(k+1|k), \\
&\hat{X}(k+1|k+1) = \hat{X}(k+1|k) + K(k+1)(Z_s(k+1) - \hat{Z}(k+1|k)), \\
&P(k+1|k+1) = P(k+1|k) - K(k+1)P_{zz}(k+1|k)K(k+1)^T,
\end{aligned}
\tag{17}
$$

where w_i^m and w_i^c are weighting factors. In this paper, $w_i^m = w_i^c = w_i$. The UKF is based on the unscented transform technique, a mechanism for propagating mean and covariance through a nonlinear transformation [29]. The state vector is approximated by a Gaussian random variable, but is represented using a minimal set of carefully chosen sample points, called sigma points. These points capture the posterior mean and covariance of the Gaussian random variable with a second order accuracy. Thus, the UKF method is supposed to have better performance in nonlinear systems.

4. Tracking results and discussion from simulation

Based on the detection chance and detection scope analysis mentioned above, a detection probability model was proposed to simulate the presence of invalid measurement in simulation. See Fig. 14. The detection probability for objects within the effective scope would always be detected precisely, saying the detection probability of 100%. Objects beyond the maximum detection scope would never been detected, which means a detection probability of 0. For objects within the maximum scope but beyond the effective scope, the detection probability would decrease linearly from 100% to 0.
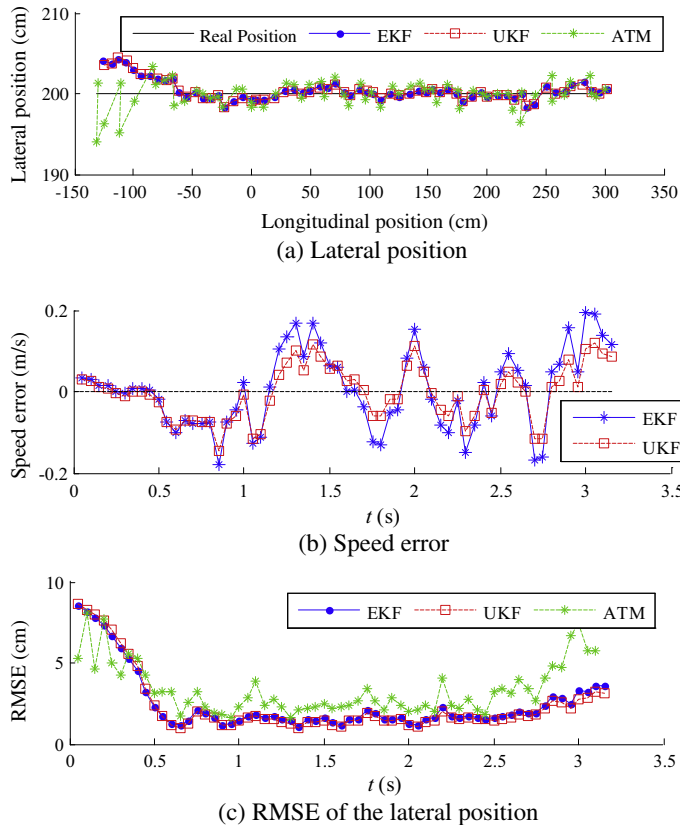

(a) Lateral position

(b) Speed error

(c) RMSE of the lateral position

Fig. 16. Tracking performance of mutual firing sequence in scenario 2.

For example, the detection capability at point T is needed. The line between T and the center (A) of the effective detection scope crosses the effective scope at point B, and extends to point C on the maximum detection scope. The detection probability at point T is r according to the model shown in Fig. 14. A random number a will be generated in the simulation experiments in Section 4 to simulate the detection capabilities of the ultrasonic sensors ($a \in [0, 1]$). If the random number a is smaller than r, the measurement at point T will be returned, which means that an object at point T will be detected. Otherwise, the object cannot be detected (no returned measurement).

An advanced triangle method (ATM) was employed to compare the tracking performance of the proposed EKF and UKF methods. The ATM calculated the mean value of the location results obtained from each pair of the 8 sensors using traditional triangle localization method. See [30–32] for more details. Three indices were used to evaluate the tracking performance of each method, including the calculated lateral position, tracking speed error and Root Mean Squared Error (RMSE) of the lateral position. See Eq. (18) for the definition of RMSE.

$$RMSE = \sqrt{\frac{1}{N} \times \sum_{i=1}^{N}(y_i - \bar{y})^2}, \tag{18}$$

where y_i is the calculated number and $\bar{y}$ is the mean value of the calculated numbers, $N = 20$.

4.1. Mutual firing sequence

For both scenarios, the proposed centralized EKF and UKF methods show better tracking capabilities with smaller RMSE compared to ATM method, especially when an object enters or exits the detection range of the arrayed ultrasonic sensors. See Figs. 15 and 16. The measured lateral distances from the three methods are very close to the ground-truth value (2 m). However, the EKF and UKF tracking results are more stable than that of the ATM method. The tracking speed errors for both EKF and UKF methods does not vary much between each other. In terms of the RMSE of the tracking lateral positions, EKF and UKF show similar results, while ATM shows larger measured differences.

4.2. Serial firing sequence

The tracking performance of serial firing sequence for scenarios 1 is shown in Fig. 17. As illustrated, the proposed centralized EKF and UKF show superior tracking ability with smaller *RMSE* compared to the ATM, especially as the tracking process

(a) Lateral position

(b) Speed error

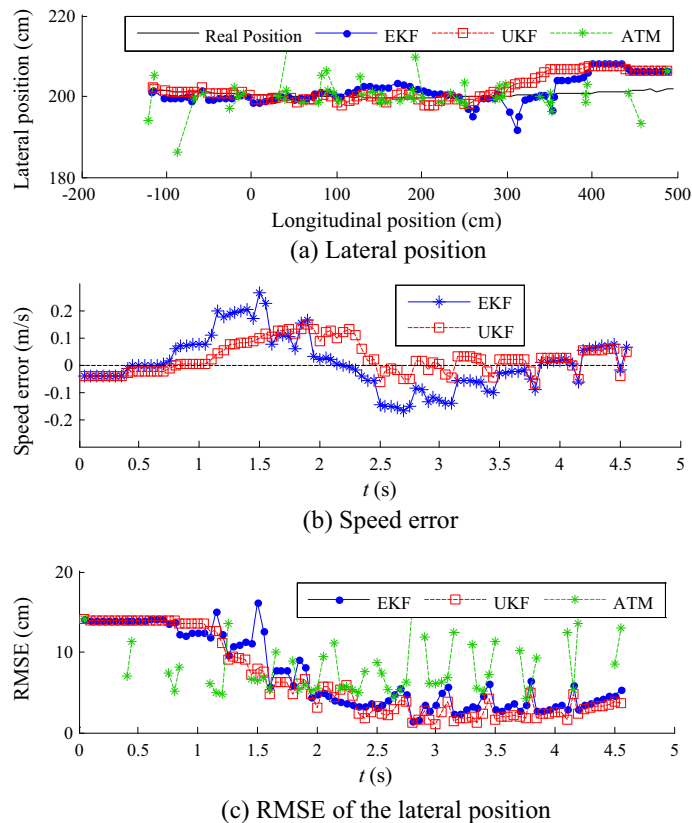(c) RMSE of the lateral position

Fig. 17. Tracking performance of serial firing sequence in scenario 1.

continues working. The proposed filters also has more stable performance with smaller volatility of *RMSE*. The proposed system and algorithms also have good speed tracking ability with a speed error less than 0.2 m/s. Under serial sensor firing sequence, UKF shows better position and speed tracking performance than the centralized EKF, because under this condition, the observation system has more nonlinear factors than that of the mutual firing sequence. Similar results were found in scenario 2.

5. Verification of the tracking algorithm from field tests

To verify the tracking performance of the proposed algorithms in real field tests, serial firing sequence was utilized to track a metal pole in the side zone. The linearly arrayed sensors were mounted on the side of a test vehicle with an interval of 50 cm between each. The height of the mounted position was 90 cm from the ground. Sound-absorbing sponges were used to avoid noise to adjacent sensors or from ground reflection. See Fig. 18(a) and (b) for the arrayed sensors and the instrumented vehicle. The test was conducted in an open test field in slight wind conditions. As shown in Fig. 18(c), a metal pole was located 1 m, 2 m, 3 m and 4 m from the side of the test vehicle sequentially. A driver drove the vehicle straight ahead with a speed of 5 km/h. The trials were repeated 5 times at each distance.

Similar with the simulation results shown in the previous section, the proposed centralized EKF and UKF algorithms showed superior tracking capability in the field test scenario shown in Fig. 18(c) using a real instrumented vehicle. See Fig. 19. Both EKF and UKF showed better position tracking capability than ATM. Concerning the tracking speed error, UKF performed better than EKF. It indicates that UKF is more suitable in the solutions to nonlinear systems. Note that the tracking speed error in the field tests was larger than the error in the simulation tests. It is probably because of the measurement accuracy of the vehicle speed (only integer numbers were allowed for recording in the field tests).

6. Conclusion and future work

This paper presents a cost-effective approach to track moving objects around vehicles using linearly arrayed ultrasonic sensors. An accurate ultrasonic detection model was developed considering the shapes and surface materials of the detected objects. For objects with the same shape, metal ones were more likely to be detected than PVC plastic ones, than cloth ones. Similarly, for objects with the same material, flat surface ones were likely to be detected than thick rods, than thin rods, due
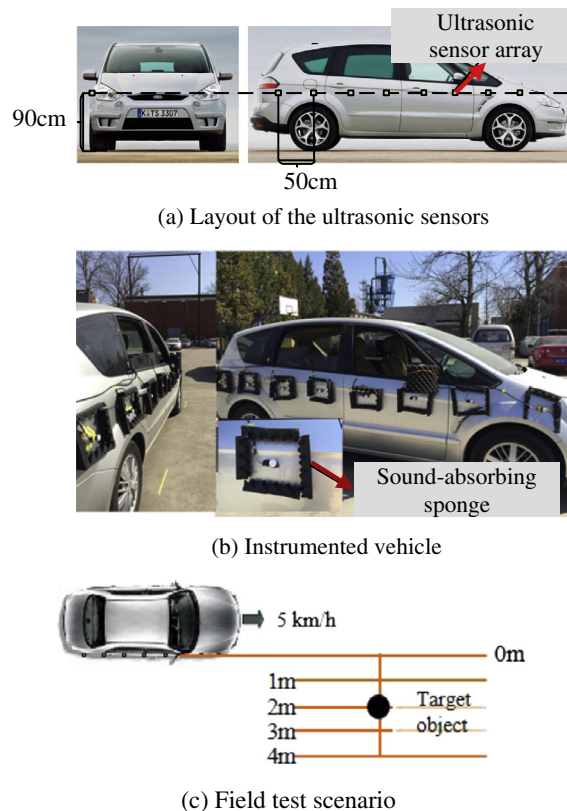

(a) Layout of the ultrasonic sensors

(b) Instrumented vehicle

(c) Field test scenario

Fig. 18. Descriptions of the field test.
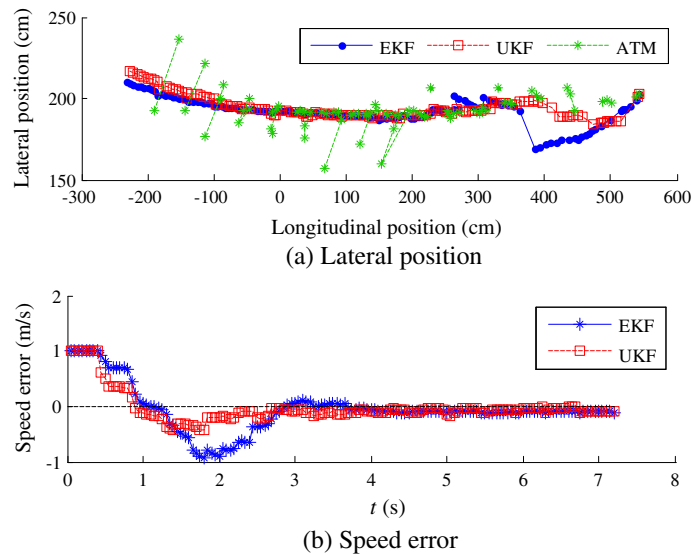
(a) Lateral position

(b) Speed error

Fig. 19. Tracking performance of serial firing sequence in a field test with a metal pole 2 m from the instrumented vehicle.

to the variance of their effective echo reflection area. Two algorithms, including an Extended Kalman filter (EKF) and an Unscented Kalman filter (UKF), were designed for object tracking based on eight linearly arrayed ultrasonic sensors. The algorithms were verified in two typical scenarios, one of which was passing by a metal pole of traffic signs or street lights and the other one was overtaking by another vehicle. The sensors would fire at the same time (mutual firing sequence) or in queue (serial firing sequence). Both EKF and UKF showed more precise tracking position and smaller RMSE (root mean square error) compared to an advanced triangle method. Although both methods performed similarly in mutual firing sequence, UKF had better performance than EKF in serial firing sequence. Thus, the proposed methods are capable of continuously tracking of both static and moving objects dynamically. The better performance of UKF indicates that UKF is more suitable in the solutions to nonlinear systems. The effectiveness of the proposed methods encourages the application of cost-effective ultrasonic sensors in the environment perception of intelligent driving systems.

The limitations of this study lie in the following two aspects: (1) The tracking capability of ultrasonic sensors studied in this paper are for low speed situations. When applied in higher speed situations, the effect of wind cannot be neglected. Thus, the measurement models of the ultrasonic sensors as well as the tracking capability of the proposed methods should be further verified and discussed. (2) The work presented in this paper focuses on the solutions to single object tracking. Only one object would appear in the detection range of the arrayed sensors at the same time. Since there would be multiple objects presented simultaneously in the detection range in real traffic, the tracking capability of the proposed methods in multiple tracking situations deserves to be analyzed in further studies. Besides, only sequential firing sequence was verified in the field tests. Effectiveness of mutual firing sequence in dynamical object tracking situations still needs to be verified in further field test studies, although it is believed to be effective from the knowledge presented in this paper.

Acknowledgement

References

[1] K. Bengler, K. Dietmayer, B. Farber, M. Maurer, C. Stiller, H. Winner, Three decades of driver assistance systems: review and future perspectives, IEEE Intell. Transp. Syst. Mag. 6 (2014) 6–22.
[2] G. Li, S. Eben Li, B. Cheng, Field operational test of advanced driver assistance systems in typical Chinese road conditions: the influence of driver gender, age and aggression, Int. J. Automot. Technol. 16 (2015) 739–750.
[3] V. Agarwal, N.V. Murali, C. Chandramouli, A cost-effective ultrasonic sensor-based driver-assistance system for congested traffic conditions, IEEE Trans. Intell. Transp. Syst. 10 (2009) 486–498.
[4] FHWA, Traffic Monitoring Guide, U.S. Department of Transportation, 2012.
[5] G. Griffin, K. Nordback, T. Götschi, E. Stolz, S. Kothuri, Monitoring Bicyclist and Pedestrian Travel and Behavior, Transportation Research Board, Washington, D.C., 2014.
[6] S. Taghvaeeyan, R. Rajamani, Portable roadside sensors for vehicle counting, classification, and speed measurement, IEEE Trans. Intell. Transp. Syst. 15 (2014) 73–83.
[7] C.-C. Tong, J.F. Figueroa, E. Barbieri, A method for short or long range time-of-flight measurements using phase-detection with an analog circuit, IEEE Trans. Instrum. Meas. 50 (2001) 1324–1328.

[8] C. Xu, P. Zhang, H. Wang, Y. Li, C. Lv, Ultrasonic echo waveshape features extraction based on QPSO-matching pursuit for online wear debris discrimination, Mech. Syst. Signal Process. 60–61 (2015) 301–315.

[9] W.-Y. Tsai, H.-C. Chen, T.-L. Liao, An ultrasonic air temperature measurement system with self-correction function for humidity, Meas. Sci. Technol. 16 (2005) 548–555.

[10] R. Kuc, M.W. Siegel, Physically based simulation model for acoustic sensor robot navigation, IEEE Trans. Pattern Anal. Mach. Intell. PAMI-9 (1987) 766–778.

[11] S. Thrun, W. Burgard, D. Fox, Probabilistic Robotics, MIT Press, Cambridge, Massachusetts, 2005.

[12] S.B. Akat, V. Gazi, L. Marques, Asynchronous particle swarm optimization-based search with a multi-robot system: simulation and implementation on a real robotic system, Turk. J. Electr. Eng. Comput. Sci. 18 (2010) 749–764.

[13] M. Ishihara, M. Shiina, S. Suzuki, Evaluation of method of measuring distance between object and walls using ultrasonic sensors, J. Asian Electric Vehicles 7 (2009) 1207–1211.

[14] J. Majchrzak, M. Michalski, G. Wiczynski, Distance estimation with a long-range ultrasonic sensor system, IEEE Sens. J. 9 (2009) 767–773.

[15] O. Wijk, H.I. Christensen, Triangulation-based fusion of sonar data with application in robot pose tracking, IEEE Trans. Robotics Automation 16 (2000) 740–752.

[16] G. Li, S.E. Li, B. Cheng, P. Green, Estimation of driving style in naturalistic highway traffic using maneuver transition probabilities, Transp. Res. Part C: Emerg. Technol. 74 (2017) 113–125.

[17] P. Köhler, C. Connette, A. Verl, Vehicle tracking using ultrasonic sensors & joined particle weighting, in: Proceedings of 2013 IEEE International Conference on Robotics and Automation (ICRA), 2013, pp. 900–2905.

[18] P. Yang, Efficient particle filter algorithm for ultrasonic sensor-based 2D range-only simultaneous localisation and mapping application, IET Wireless Sensor Syst. 2 (2012) 394–401.

[19] W. Adiprawita, A.S. Ahmad, J. Sembiring, B.R. Trilaksono, New resampling algorithm for particle filter localization for mobile robot with 3 ultrasonic sonar sensor, in: Proceedings of 2011 International Conference on Electrical Engineering and Informatics (ICEEI), 2011.

[20] L. Zhang, R. Zapata, Probabilistic localization methods of a mobile robot using ultrasonic perception system, in: Proceedings of 2009 International Conference on Information and Automation, 2009, pp. 062–1067.

[21] J. Muller, A. Rottmann, L.M. Reindl, W. Burgard, A probabilistic sonar sensor model for robust localization of a small-size blimp in indoor environments using a particle filter, in: Proceedings of 2009 IEEE International Conference on Robotics and Automation, 2009, pp. 589–3594.

[22] L. D'Alfonso, W. Lucia, P. Muraca, P. Pugliese, Mobile robot localization via EKF and UKF: a comparison based on real data, Robotics Autonomous Syst. 74 (2015) 122–127.

[23] S.I. Ko, J.S. Choi, Indoor mobile localization system using UKF and pre-filtering, in: Proceedings of 2007 IEEE/RSJ International Conference on Intelligent Robots and Systems, 2007, pp. 865–2870.

[24] S.J. Kim, B.K. Kim, Dynamic ultrasonic hybrid localization system for indoor mobile robots, IEEE Trans. Industr. Electron. 60 (2013) 4562–4573.

[25] S.E. Li, S. Xu, X. Huang, B. Cheng, H. Peng, Eco-departure of connected vehicles with V2X communication at signalized intersections, IEEE Trans. Veh. Technol. 64 (2015) 5439–5449.

[26] K.-W. Jörg, M. Berg, Sophisticated mobile robot sonar sensing with pseudo-random codes, Robotics Autonomous Syst. 25 (1998) 241–251.

[27] E.A. Wan, R. Van Der Merwe, The unscented Kalman filter for nonlinear estimation, in: Proceedings of 2000 IEEE Adaptive Systems for Signal Processing, Communications, and Control Symposium, 2000, pp. 53–158.

[28] S.J. Julier, J.K. Uhlmann, H.F. Durrant-Whyte, A new approach for filtering nonlinear systems, in: Proceedings of 1995 American Control Conference, 1995, pp. 628–1632.

[29] K. Xiong, H.Y. Zhang, C.W. Chan, Performance evaluation of UKF-based nonlinear filtering, Automatica 42 (2006) 261–270.

[30] J. Borenstein, Y. Koren, Obstacle avoidance with ultrasonic sensors, IEEE J. Robotics Automation 4 (1998) 213–218.

[31] J.J. Leonard, H.F. Durrant-Whyte, Mobile robot localization by tracking geometric beacons, IEEE Trans. Robotics Automation 7 (1991) 376–382.

[32] S.S. Ghidary, T. Tani, M. Takamori, A. Hattori, A new Home Robot Positioning System (HRPS) using IR switched multi ultrasonic sensors, in: Proceedings of 1999 IEEE International Conference on Systems, Man, and Cybernetics, 1999, pp. 737–741.